DYNAMIC EFFECTS IN MODE III CRACK BIFURCATION

JOHN P. DEMPSEY

Department of Civil and Environmental Engineering, Clarkson University, Potsdam,
NY 13676, U.S.A.

MAO-KUEN KUO

Institute of Applied Mechanics, College of Engineering, National Taiwan University, Taipei,
Taiwan

and

DIANE L. BENTLEY

Department of Civil and Environmental Engineering, Clarkson University, Potsdam,
NY 13676, U.S.A.

Abstract—Transient elastodynamic nonplanar self-similar Mode III crack growth in brittle materials is examined. The dynamic similarity and Chaplygin's transformation reduce the class of problems considered to the solution of Laplace's equation in a semi-infinite strip. The Schwarz–Christoffel transformation is subsequently employed to map the semi-infinite strip on a half-plane. The theory of analytic functions can then be used. Elastodynamic influences in the vicinity of a rapidly moving tip after branching are examined in a rather general fashion.

To reveal the sensitivity of one branch's crack tip elastodynamic stress intensity factor to the relative velocity and orientation of the other, the problem of asymmetric crack bifurcation under stress wave loading is chosen for study. The development of specific analytical solutions requires the solutions to the symmetric bifurcation problem subjected to loading that induces either antisymmetrical or symmetrical deformations, respectively, about the original crack plane. For asymmetric geometries the solution required the numerical evaluation of several integrals in the final stages. It is ultimately shown that the stress intensity factor of one branch is significantly altered by changes in the velocity and orientation of the other and by the angle of stress wave incidence.

1. INTRODUCTION

Dynamic fracture in brittle solids is characterized by the rapid attainment of high crack tip velocities and the tendency thereafter to branch, propagate further and branch, and so on (Schardin[1]; Clark and Irwin[2]; Dally[3]). An interesting high-speed photomicrographic study of the evolution of crack branching by Ravi-Chandar and Knauss[4] revealed that there is no single instant of crack branch initiation and that there are multiple branching attempts made by the propagating crack. A marked increase in surface roughness usually heralds crack branching. Present elastodynamic treatments have great difficulty incorporating any of the microscopic details and the fact that nonsynchronous branching occurs. The approximations to planar deformations and through-the-thickness straight-front crack propagation are therefore not unreasonable. The assumption that small-scale yielding conditions prevail is also not unreasonable since brittle fracture is involved. In other words, the process zone—the region in which the crack rapidly curves—is assumed to be small in size with respect to any characteristic length in the problem. The latter assumption is valid for glass and rock as well as the not-so-brittle materials such as polymers and steel that are subjected to low-temperature environments and/or high rates of loading. Analytically the process zone is modelled as a point, giving a well-defined instant of branching.

Dynamic crack branching has been observed in a variety of materials including glass plates and pressurized tubes (Schardin[1], Aoki and Sakata[5]), steel plates and pressurized steel and aluminum pipes (Hahn, Hoagland and Rosenfield[6], Congleton[7], Kobayashi[8]), crystalline solids (Field[9]), rock (Bienawski[10]), and brittle polymers such as Homalite-100 (Dally[3], Ravi-Chandar and Knauss[4], Kobayashi, Wade, Bradley and Chiu[11], Ramulu, Kobayashi and Kang[12]). The angle subtended

by the macroscopic branch—immediately after branching—and the original crack plane typically lies between 10° to 45° for the more brittle materials that have no preferred orientations. The speed of crack tip propagation, which is usually less than half the shear wave speed, is not significantly influenced by the branching event.

Much of the analytical work dealing with crack branching under an arbitrary angle with the primary crack is elastostatic in nature. For antiplane strain deformations, the infinite body with a kinked and bifurcated crack were presented by Sih[13] and Smith[14], respectively. The equivalent elastostatic in-plane problems were treated by Lo[15]; multiple branching (Wilson and Cherepko[16]) and successive bifurcation (Parletun[17]) have been investigated using the finite element method. The slow growth of cracks in nonuniform stress fields, with no a priori assumption regarding the path of the crack branch, has been examined using perturbation procedures by Banichuk[18], Cotterell and Rice[19], and Karihaloo, Keer, Nemat-Nasser and Oranratnachai[20]. There have been proposals to determine the conditions for crack branching from the stress–strain field for the unbranched crack (the prior field). The use of the prior stress field criteria (Maiti and Smith[21]) may be useful if the path of fracture is not likely to cause a significant readjustment of the prior stress field.

Experimental observations of the speed of crack propagation at branching suggest that elastodynamic effects are important. The fact that the $\sigma_{\theta\theta}$ stress moves out of the plane of crack propagation and acts at an angle of about 60° to the direction of crack propagation when the crack velocity exceeds approximately 0.6 times the shear wave velocity (Yoffe[22], Craggs[23]) reinforces the view that inertia effects are important.

The treatment of the fast growth of cracks in nonuniform stress fields, with no a priori assumption regarding the crack path, has as yet eluded current research efforts. An alternative approach is to determine a necessary condition prior to crack branching by comparing states prior to and after branching. The comparison requires expressions for the elastodynamic field quantities near the tips of the branches. The necessary condition can then be established, for instance, on the basis of the balance of the rates of energies.

A problem fundamental to our understanding of the conditions for dynamic crack branching in brittle solids is the sudden kinking or bifurcation of a running crack. In this paper the transient diffraction of an elastic wave by an extending but bifurcating crack is considered. The incident wave is a plane horizontally polarized wave. It is assumed that crack division is generated at the instant that the tip of a stationary crack is struck. The original length of the crack is therefore immaterial for small times, and the analytical work can be simplified by considering a semi-infinite crack. Size effects become important for later times. The two new crack tips are assumed to propagate at different but constant velocities under different but arbitrary angles with the original crack plane. The dependence of the elastodynamic stress intensity factors on the crack-tip velocities and the angles of branching is examined.

The solution method used in this paper is based on the observation that for a class of externally applied disturbances the particle velocity is self-similar within the circular regions of the diffracted wave. The fact that $\dot{w}$, for constant crack-tip velocities, is a function of r/t and θ only allows Chaplygin's transformation to be used, which reduces the problem to the solution of Laplace's equation in a semi-infinite strip containing two slits. The Schwarz–Christoffel transformation is subsequently employed to map the semi-infinite strip on a half-plane. The powerful theory of analytic functions (Muskhelishvili[24]) can then be used.

Transient elastodynamic nonplanar self-similar crack growth solutions have only recently been obtained. Burgers and Dempsey[25] solved the symmetric crack bifurcation problem in antiplane strain for a specific angle, while Dempsey, Kuo and Achenbach[26] solved the Mode III crack kinking problem for stress wave loading. The latter solutions provided much-needed check cases for the numerical method being applied by Burgers[27, 28] and Burgers and Dempsey[29]. Skew crack propagation (Achenbach and Varatharajulu[30]) and crack bifurcation (Achenbach[31, 32], Freund[33]) were first examined a decade ago; these studies helped to establish the

viability of the approach used in the more recent studies mentioned above and in this paper.

In Section 2, self-similar solutions to the class of problems considered are formulated and the elastodynamic influences on the stresses and the particle velocity in the vicinity of a rapidly moving crack tip are examined in a rather general fashion. The universal spatial dependence of the near tip stress field and particle velocity field is revealed, as is the fact that the only problem-dependent quantity is the stress intensity factor. The problem of asymmetric crack bifurcation under stress wave loading is formulated in Section 3. Symmetric crack bifurcation under loading conditions that induce solely antisymmetric or symmetric deformations is solved in Section 4, prior to solving for symmetric crack bifurcation under stress wave loading (with equal crack-tip velocities). The general asymmetric crack bifurcation problem is solved in Section 5 for stress wave loading. To gain an increased understanding of the dynamic crack branching mechanism, and also to examine the attempted branching during the planar phase of crack propagation, several asymmetric bifurcation geometries are chosen. The objective is to determine the sensitivity of one branch's crack-tip elastodynamic stress intensity factor to the relative velocity and orientation of the other. Elastostatic studies that have had a similar purpose include those by Parletun[17] and Kalthoff[34].

2. SELF-SIMILAR SOLUTIONS

In a stationary system of polar coordinates (r, θ), two-dimensional antiplane wave motions are governed by

$$\frac{1}{r} \frac{\partial}{\partial r} \left(r \frac{\partial w}{\partial r} \right) + \frac{1}{r^2} \frac{\partial^2 w}{\partial \theta^2} = \frac{1}{c^2} \ddot{w}, \tag{2.1}$$

where $w(r, \theta, t)$ is the out-of-plane displacement, $(\dot{\ }) = \partial/\partial t$, and $c = (\mu/\rho)^{1/2}$ is the velocity of transverse waves. The relevant shear stresses are

$$\tau_{rz} = \mu \frac{\partial w}{\partial r}, \qquad \tau_{\theta z} = \frac{\mu}{r} \frac{\partial w}{\partial \theta}. \tag{2.2a,b}$$

For geometrical configurations without a fixed characteristic length and with appropriate boundary conditions, either $w(r, \theta, t)$ or $\dot{w}(r, \theta, t)$ may display the property of self-similarity. In this paper, we will consider cases in which the particle velocity, $\dot{w}(r, \theta, t)$, is self-similar. This implies that $\dot{w}$ depends on r/t and θ, rather than on θ, r and t separately. On introducing the new variable $s = r/t$, the equation for $\dot{w}(s, \theta)$ follows from (2.1) as

$$s^2 \left(1 - \frac{s^2}{c^2} \right) \frac{\partial^2 \dot{w}}{\partial s^2} + s \left(1 - \frac{2s^2}{c^2} \right) \frac{\partial \dot{w}}{\partial s} + \frac{\partial^2 \dot{w}}{\partial \theta^2} = 0. \tag{2.3}$$

For $s < c$, Chaplygin's transformation $\beta = \cosh^{-1}(c/s)$ reduces (2.3) to Laplace's equation

$$\frac{\partial^2 \dot{w}}{\partial \beta^2} + \frac{\partial^2 \dot{w}}{\partial \theta^2} = 0, \qquad \beta = \cosh^{-1} \left(\frac{c}{s} \right). \tag{2.4a,b}$$

The real transformation given by (2.4b) maps the interior of the physical domain into a semi-infinite strip in the γ-plane. In this plane the harmonic function $\dot{w}(\beta, \theta)$ can be taken as the real part of an analytic function $G(\gamma)$, $\gamma = \beta + i\theta$. Formally, $G(\gamma)$ can be obtained by conformal mapping techniques, whereby the domain in the γ-plane is mapped on the upper half of the ζ-plane by means of a Schwarz–Christoffel

transformation:

$$\gamma = \omega(\zeta), \qquad \zeta = \xi + i\eta. \tag{2.5a,b}$$

In the ζ-plane the solution is of the form

$$\dot{w} = \mathrm{Re}\, F(\zeta), \tag{2.6}$$

where $F(\zeta)$ must be obtained from the boundary conditions on the real axis. By the use of (2.6), (2.2) and (2.4b), the stress components are given by

$$\tau_{rz} = \mu\, \mathrm{Re} \int_{r/c}^{t} \left[F'(\bar{\zeta}) \frac{d\bar{\zeta}}{d\bar{\gamma}} \frac{\partial\bar{\gamma}}{\partial\bar{\beta}} \frac{\partial\bar{\beta}}{\partial r} \right] d\bar{t} + \tau_{rz}^{w}, \tag{2.7}$$

$$\tau_{\theta z} = \frac{\mu}{r}\, \mathrm{Re} \int_{r/c}^{t} \left[F'(\bar{\zeta}) \frac{d\bar{\zeta}}{d\bar{\gamma}} \frac{\partial\bar{\gamma}}{\partial\theta} \right] d\bar{t} + \tau_{\theta z}^{w}, \tag{2.8}$$

where τ_{rz}^{w} and $\tau_{\theta z}^{w}$ are the values of τ_{rz} and $\tau_{\theta z}$ for $r > ct$.

The crucial part of the analysis of any self-similar problem is the derivation of $F'(\zeta)$. The completeness of this function must be established: terms which violate the boundary conditions or introduce inadmissible singularities must not be included. The relationship between ζ and the physical coordinates r/t and θ given in (2.5a) is generally not invertible for problems involving dynamic crack branching. The incorporation of the appropriate singular behavior in a particular problem through $F'(\zeta)$ hinges upon establishing the relations between small distances from the crack tip in the physical plane, in the γ-plane, and in the ζ-plane.

Without discussing a particular problem at this stage, consider a crack that starts propagating at $t = 0$ with constant velocity, v, from the origin of a Cartesian coordinate system in the x, y-plane under an angle $\kappa\pi$ with the x-axis. At any instant, the length of the crack is vt, and its motion can be described by the conventional cylindrical coordinates r, θ, z centered at the origin, or the coordinates ρ, ϕ, z centered at the crack tip (Fig. 1).

For small values of ρ/vt (see Fig. 1) the following relations can be derived, using $m = v/c$,

$$\theta - \kappa\pi \sim (\rho/vt)\sin(\phi), \tag{2.9a}$$

$$r - vt \sim \rho\cos(\phi), \tag{2.9b}$$

$$\beta - \beta_D \sim -\frac{(\rho/vt)\cos(\phi)}{(1 - m^2)^{1/2}}. \tag{2.9c}$$

We find from (2.5a) that for $|\zeta - \xi_D| \ll 1$ and $\kappa \neq 0$

$$\gamma - \gamma_D \sim \omega_2(\zeta - \xi_D)^2/2, \tag{2.10}$$

where ω_2 is a constant that depends on the particular mapping used and $\gamma_D = \beta_D + i\kappa\pi$. Equations (2.9c) and (2.10) give for ρ/vt small and $\kappa \neq 0$

$$\zeta - \xi_D \sim (\rho/vt)^{1/2}[Z_1(\phi, m) + iZ_2(\phi, m)]Q(\kappa, \phi, m), \tag{2.11}$$

where

$$Z_1(\phi, m) = \mathrm{sgn}(\phi)\{[1 - m^2\sin^2(\phi)]^{1/2} - \cos(\phi)\}^{1/2}/[1 - m^2\sin^2(\phi)]^{1/2}, \tag{2.12a}$$

$$Z_2(\phi, m) = \{[1 - m^2\sin^2(\phi)]^{1/2} + \cos(\phi)\}^{1/2}/[1 - m^2\sin^2(\phi)]^{1/2}, \tag{2.12b}$$

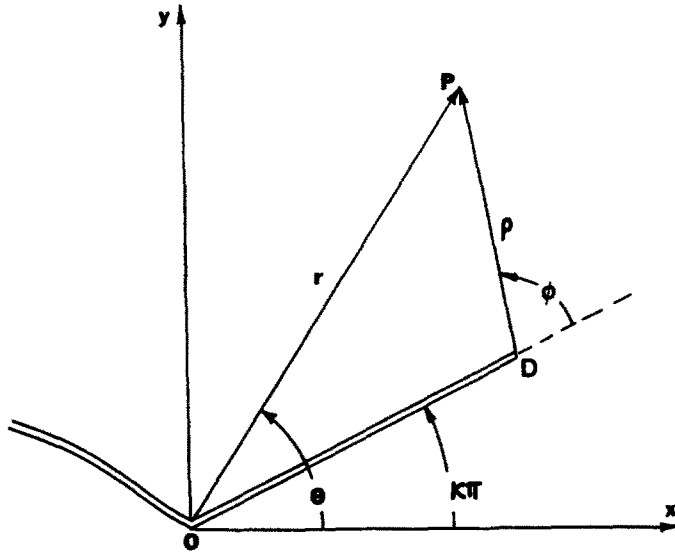$$Q(\kappa, \phi, m) = [1 - m^2\sin^2(\phi)]^{1/2}/\omega_2^{1/2}(1 - m^2)^{1/4}. \tag{2.12c}$$

Fig 1. Polar coordinates centered at the moving crack tip

It is apparent from (2.11) that for $\kappa \neq 0$ a singularity of order $(r - vt)^{-1/2}$ in the particle velocity (2.6) corresponds to a singularity of order $(\zeta - \xi_D)^{-1}$ in $F(\zeta)$. In other words, since $\dot{\tau}_{\theta z}$ is singular as $(r - vt)^{-3/2}$ in the vicinity of the propagating tip, then $F'(\zeta)$ $(d\zeta/d\gamma)$ must harbor the term $(\zeta - \xi_D)^{-3}$ for small $|\zeta - \xi_D|$.

For the class of problems under consideration, a convenient way to express $F'(\zeta)$ is in the form

$$F'(\zeta) = F_1'(\zeta) + F_2'(\zeta), \tag{2.13}$$

in which $F_1'(\zeta)$ satisfies the nonhomogeneous boundary conditions in the ζ-plane on the real axis, while $F_2'(\zeta)$ incorporates the singular behavior at the crack-tip. Using (2.13), the stress components (2.7) and (2.8) can be expressed in the form

$$\tau_{pz} = \{I_{1p}(s, \theta) + I_{2p}(s, \theta)\}H(c - s) + \tau_{pz}^w, \qquad (p = r, \theta), \tag{2.14}$$

in which, for $k = 1$ or 2,

$$I_{kr} = -\mu \, \mathrm{Re} \int_s^c F_k'(\bar{\zeta}) \frac{d\bar{\zeta}}{d\bar{\gamma}} \frac{d\bar{s}}{\bar{s}^2(1 - \bar{s}^2/c^2)^{1/2}}, \tag{2.15a}$$

$$I_{k\theta} = -\mu \, \mathrm{Im} \int_s^t F_k'(\bar{\zeta}) \frac{d\bar{\zeta}}{d\bar{\gamma}} \frac{d\bar{s}}{\bar{s}^2}. \tag{2.15b}$$

Except for special cases, an explicit expression for $\bar{\zeta}$ in terms of $\bar{s}$ and θ cannot be obtained from the Schwarz–Christoffel transformation. Before doing the above integration numerically, the singular term in I_{2r} and $I_{2\theta}$ must be treated analytically. To this end the integration over $\bar{s}$ is replaced by an integration over a corresponding contour Γ in the ζ-plane. The appropriate changes of variables gives

$$I_{2r} = \frac{\mu}{c} \, \mathrm{Re} \int_\Gamma F_2'(\bar{\zeta}) \cosh \beta(\bar{\zeta}) \, d\bar{\zeta}, \tag{2.16}$$

$$I_{2\theta} = \frac{\mu}{c} \, \mathrm{Im} \int_\Gamma F_2'(\bar{\zeta}) \sinh \beta(\bar{\zeta}) \, d\bar{\zeta}. \tag{2.17}$$

Integrating (2.16) and (2.17) by parts, the final expressions for the stress components

are

$$\tau_{rz}(s, \theta) = \left\{ -\frac{\mu}{\bar{s}} \text{ Re } F_2(\bar{\zeta}) \big|_{s=s} + \frac{\mu}{c} \text{ Re } F_2(\bar{\zeta}) \big|_{\bar{s}=c} \right.$$

$$\left. + J_{2r}(s, \theta) + I_{1r}(s, \theta) \right\} H(c - s) + \tau_{rz}^u, \qquad (2\ 18)$$

$$\tau_{\theta z}(s, \theta) = \left\{ -\frac{\mu}{\bar{s}} \left(1 - \frac{\bar{s}^2}{c^2} \right)^{1/2} \text{ Im } F_2(\bar{\zeta}) \big|_{\bar{s}=s} \right.$$

$$\left. + J_{2\theta}(s, \theta) + I_{1\theta}(s, \theta) \right\} H(c - s) + \tau_{\theta z}^u, \qquad (2.19)$$

in which

$$J_{\lambda r} = \mu \text{ Re } \int_{s}^{c} F_\lambda(\bar{\zeta}) \frac{d\bar{s}}{\bar{s}^2}, \qquad (2.20)$$

$$J_{\lambda \theta} = \mu \text{ Im } \int_{s}^{c} F_\lambda(\bar{\zeta}) \frac{d\bar{s}}{\bar{s}^2(1 - \bar{s}^2/c^2)^{1/2}}. \qquad (2.21)$$

Here $\bar{\zeta}$ is considered as a functiion of $\bar{s}$, which in general cannot be determined explicitly. For any value of $\bar{s}$ the corresponding $\bar{\zeta}$ can be computed numerically from (2.5a).

In any particular problem, the Mode III stress intensity factor must be determined by considering the shear stress $\tau_{\theta z}$ in the plane of the crack, and ahead of the crack tip, since

$$K_{III} = \lim_{r \to vt} (2\pi)^{1/2}(r - vt)^{1/2}\tau_{\theta z}(r > vt, \theta = \kappa\pi). \qquad (2.22)$$

The elastodynamic influences on the stresses and the particle velocity in the vicinity of the moving crack tip in problems involving crack branching under dynamic loading conditions are also of interest here. For this reason let the state of stress at point P in Fig. 1 be given by both $(\tau_{rz}, \tau_{\theta z})$ and $(\tau_{\rho z}, \tau_{\phi z})$, where it can be shown that

$$\tau_{\phi z} = -\tau_{rz} \sin(\phi - \theta + \kappa\pi) + \tau_{\theta z} \cos(\phi - \theta + \kappa\pi). \qquad (2.23)$$

Equation (2.23) along with eqns (2.18), (2.19) and (2.11), can be used to investigate the stresses in the vicinity of the crack tip, which reveals that for small ρ/vt,

$$\tau_{\phi z} \sim -(\mu/v) \{(1 - m^2)^{1/2} \text{ Im } F_2(\bar{\zeta}) \big|_{\bar{s}=s} \cos(\phi) - \text{ Re } F_2(\bar{\zeta}) \big|_{\bar{s}=s} \sin(\phi)\}. \quad (2.24)$$

The above equation reduces to the same expression for all problems in the class discussed in this paper. That is, for ρ/vt small,

$$\tau_{\phi z} \sim T_{\phi z}(\phi, m) K_{III}/(2\pi\rho)^{1/2}, \qquad (2.25)$$

where

$$T_{\phi z}(\phi, m) = \{(1 - m^2)^{-1/2}Z_1(\phi, m) \sin(\phi) + Z_2(\phi, m) \cos(\phi)\}/2^{1/2}, \qquad (2.26)$$

in which $Z_{1,2}(\phi, m)$ are defined in (2.12a,b). The dependence of the local shear stress, $\tau_{\phi z}$, on the problem at hand is incorporated into one term, the stress intensity factor. The dependence of the local shear stress on the polar angle in the vicinity of the moving crack tip is incorporated in $T_{\phi z}$; as shown by Erdogan[35], the maximum value of $T_{\phi z}$ moves out of the plane of crack propagation ($\phi = 0$) as the crack velocity increases

beyond a certain critical value ($m = 3^{-1/2} \approx 0.578$). Obviously, even after a crack has branched, the maximum value of the shear stress may not be maintained in the new plane of crack propagation. For various values of m, the variation of $\sqrt{2}\, T_{\phi z}$ in ϕ is shown in Fig. 2 of the paper by Achenbach[31] (note that ϕ in [31] is $\pi - \phi$ here); for $m \rightarrow 0$, $T_{\phi z} = \cos(\phi/2)$, and (2.25) reduces to the expression for static loading, $\tau_{\phi z} = \cos(\phi/2)\, K_{III}/(2\pi\rho)^{1/2}$.

An analogous result holds for the particle velocity, for which

$$\dot{w} \sim \frac{(c/\mu)\, W_{\phi z}(\phi, m)\, K_{III}}{(\pi\rho)^{1/2}}, \qquad (2.27)$$

where

$$W_{\phi z}(\phi, m) = mZ_1(\phi, m)/2(1 - m^2)^{1/2}. \qquad (2.28)$$

The above results are not surprising since similar results were found for mixed-mode crack propagation by Freund and Clifton[36], although in their analysis the crack-
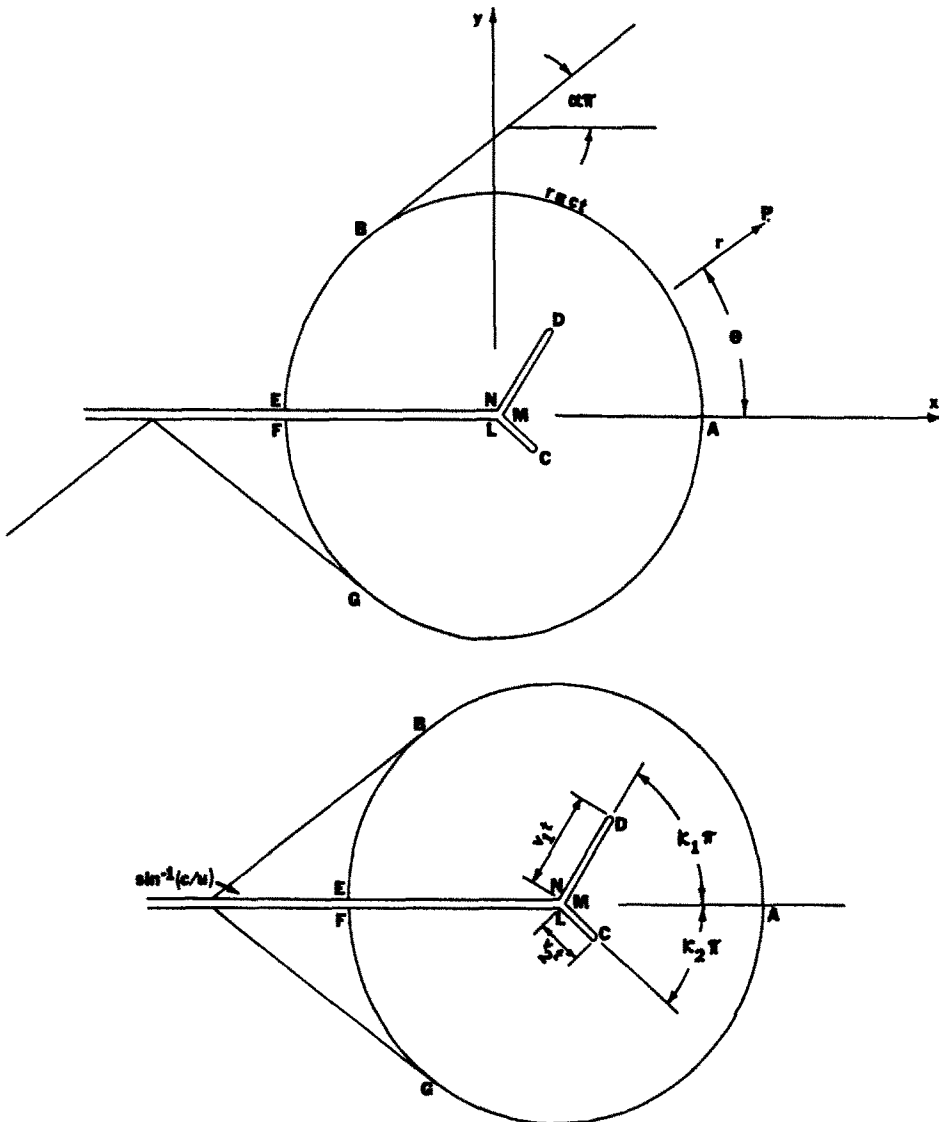

Fig. 2. (a) Pattern of incident, reflected and diffracted waves for an incident horizontally polarized transverse wave and asymmetric crack bifurcation: $\alpha\pi$ = angle of wave incidence; (b) pattern of waves for the superposition problem: $\kappa_i\pi$ = bifurcation angles, v_i = crack-tip speeds.

tip trajectory was required to have a continuously turning tangent. Even after branching, the near-tip elastodynamic fields have a universal spatial dependence on the local coordinate system. The problem-dependent quantity is the stress intensity factor. Furthermore, since the spatial dependence on the local coordinates is the same as for planar crack propagation, the flux of energy, F, into the crack tip is also known (Freund[37]):

$$F = \frac{(c/\mu)mK_{\text{III}}^2}{2(1 - m^2)^{1/2}} \, .$$ (2.29)

The balance of rates of energies (Achenbach[32]) provides a necessary condition for crack propagation. A criterion for crack branching follows if the energy release rate for the branched crack is greater than that for planar crack propagation. Clearly, the dependence of the elastodynamic stress intensity factor on the branching angle $\kappa\pi$ and crack-tip velocity v is of fundamental importance.

3. CRACK BIFURCATION UNDER STRESS WAVE LOADING

The problem to be considered in this section involves the dynamic loading of an initially stationary, semi-infinite crack by an obliquely incident horizontally polarized step stress wave. At the instant of the crack tip being struck ($t = 0$), two cracks propagate out of the original crack tip, with constant subsonic crack-tip velocities v_1 and v_2, making angles $\kappa_1\pi$ and $\kappa_2\pi$ with the original crack plane, respectively. The original crack generates a plane reflected wave and a cylindrical diffracted wave. The pattern of wavefronts and the positions of the crack tips for $t > 0$ are shown in Fig. 2(a).

The reflection and diffraction of the incident wave involve horizontally polarized motions only. The governing equation of motion is given by (2.1). The incident wave is of the form

$$w_{\text{inc}} = - (c\tau_0/\mu)\tau H(\tau),$$ (3.1)

where

$$\tau = t + (x/c) \sin(\alpha\pi) - (y/c) \cos(\alpha\pi) = t + (r/c) \sin(\alpha\pi - \theta),$$ (3.2)

and α, r and θ are defined in Fig. 2(a). The stress $\tau_{\theta z}$ corresponding to the incident wave is

$$\tau_{\theta z}^{\text{inc}} = \tau_0 \cos(\alpha\pi - \theta)H(\tau).$$ (3.3)

The total field [illustrated in Fig. 2(a)] can be considered as the superposition of the incident wave in an unbounded medium and the superposition problem. The superposition problem [Fig. 2(b)] concerns an initially quiescent solid which contains a semi-infinite crack. At time $t = 0$, two branches emanate from the crack tip, and at the same time the old and new crack faces are subjected to crack face tractions which are opposite in sign to the stresses induced by the incident wave. The superposition of the fields due to the incident wave and the superposition problem renders the crack faces free of tractions.

In this paper we solve the superposition problem. Thus, the conditions on the crack faces are

$$\theta = \pm \pi, \quad r > 0: \qquad \tau_{\theta z} = \tau_0 \cos(\alpha\pi) \, H[t + (x/c) \sin(\alpha\pi)],$$ (3.4)

$$\theta = \kappa_1\pi \pm 0, \quad r > 0: \qquad \tau_{\theta z} = - \tau_0 \cos(\alpha\pi - \kappa_1\pi) \, H(t - r/v_1),$$ (3.5)

$$\theta = \kappa_2\pi \pm 0, \quad r > 0: \qquad \tau_{\theta z} = - \tau_0 \cos(\alpha\pi - \kappa_2\pi) \, H(t - r/v_2).$$ (3.6)

The shear tractions on $\theta = \pm \pi$ generate plane waves with constant particle velocities of magnitude $\pm c\tau_0/\mu$. Thus, along the segments BE and FG of Fig. 2(b) the particle velocities are

$$\pi/2 + \alpha\pi < \theta \le \pi, \quad r = ct: \quad \dot{w} = c\tau_0/\mu, \tag{3.7}$$

$$-\pi \le \theta < -\pi/2 - \alpha\pi, \quad r = ct: \quad \dot{w} = -c\tau_0/\mu. \tag{3.8}$$

The material is undisturbed ahead of the segment BG, and thus

$$-\pi/2 - \alpha\pi < \theta < \pi/2 + \alpha\pi, \quad r = ct: \quad \dot{w} = 0. \tag{3.9}$$

Before obtaining the solution to the above asymmetric bifurcation problem, it is desirable to solve the symmetric crack bifurcation problem ($\kappa_1 = -\kappa_2 = \kappa$) for the case of equal and constant crack-tip velocities ($v_1 = v_2 = v$). The latter solution is useful both for checking purposes and for insight into the more difficult asymmetric bifurcation analysis. Moreover, the above symmetric bifurcation problem is interesting since it can be formulated as the sum of an antisymmetric problem and a symmetric problem. The antisymmetric problem is defined by the conditions in (3.4), (3.7)–(3.9) and

$$\theta = \pm \kappa\pi, \quad r > 0: \quad \tau_{\theta z} = -\tau_0 \cos(\alpha\pi) \cos(\kappa\pi)H(t - r/v), \tag{3.10}$$

$$\theta = 0, \quad r < ct: \quad \dot{w} = 0. \tag{3.11}$$

The symmetric problem is defined by the loading

$$\theta = \pm \pi, \quad r > 0: \quad \tau_{\theta z} = 0, \tag{3.12}$$

$$\theta = \pm \kappa\pi, \quad r > 0: \quad \tau_{\theta z} = \mp \tau_0 \sin(\alpha\pi) \sin(\kappa\pi)H(t - r/v), \tag{3.13}$$

$$-\pi \le \theta \le \pi, \quad r = ct: \quad \dot{w} = 0, \tag{3.14}$$

$$\theta = 0, \quad r < ct: \quad \dot{w} \ne 0, \quad \partial\dot{w}/\partial\theta = 0. \tag{3.15}$$

The above problems are solved in Section 4 in considerable detail and generality. The asymmetric problem is treated in Section 5.

4. SYMMETRIC CRACK BIFURCATION

Antisymmetrical deformations

Geometrically symmetric crack bifurcation with equal, constant crack-tip velocities and dynamic loading conditions that cause antisymmetric deformations about the original crack plane are studied here. The boundary conditions are

$$\theta = \pm \pi, \quad r > 0: \quad \tau_{\theta z} = \tau_0^s H(t + x/u), \tag{4.1}$$

$$\theta = \pm \kappa\pi, \quad r > 0: \quad \tau_{\theta z} = -\tau_1^a H(t - r/v). \tag{4.2}$$

Two plane waves and a cylindrical wave are generated by this loading. The pattern of waves is shown in Fig. 2(b) (assuming that $\kappa_1 = -\kappa_2 = \kappa$, $v_1 = v_2 = v$). In the following analysis it is assumed that $u > c$.

The dynamic shear tractions in (4.1) generate plane waves. In the regions outside the cylindrical wavefront $r = ct$ and behind these plane waves the particles velocities are of constant magnitude, such that along arcs BE and FG,

$$\pi/2 + \sin^{-1}(1/n) \le \pm\theta \le \pi, \quad r = ct: \quad \dot{w} = \frac{\pm(c\tau_0^s/\mu)n}{(n^2 - 1)^{1/2}}, \tag{4.3}$$

where

$$n = u/c, \qquad n > 1. \tag{4.4}$$

The material ahead of BG is undisturbed:

$$|\theta| < \pi/2 + \sin^{-1}(1/n), \quad r = ct: \qquad \dot{w} = 0, \quad \partial\dot{w}/\partial\theta = 0. \tag{4.5}$$

The line $\theta = 0$ is a line of antisymmetry:

$$\theta = 0, \quad 0 < r < ct: \qquad \dot{w} = 0, \quad \partial\dot{w}/\partial r = 0. \tag{4.6}$$

As outlined in Section 2 the above antisymmetric problem is mapped from the physical domain ($0 \leq \theta \leq \pi$, $s \leq c$) into a semi-infinite strip ($0 \leq \theta \leq \pi$, $0 < \beta < \infty$) in the γ-plane (Fig. 3). This strip is then mapped to the upper half of the ζ-plane (Fig. 4) by the Schwarz–Christoffel transformation (Achenbach[32]):

$$\gamma = \kappa \cosh^{-1}\left(\frac{1 + \zeta\xi_M}{\zeta + \xi_M}\right) + (1 - \kappa)\cosh^{-1}\left(\frac{1 - \zeta\xi_N}{\zeta - \xi_N}\right) + i\pi, \tag{4.7}$$

where the points ξ_M, ξ_N and ξ_B can be found, for given values of κ and m, by considering the change in imaginary parts at M and N between the γ-plane and ζ-plane, and from
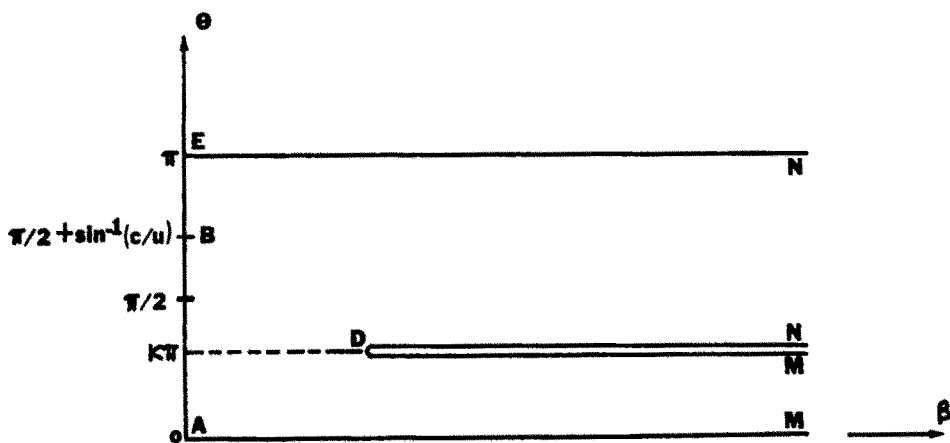

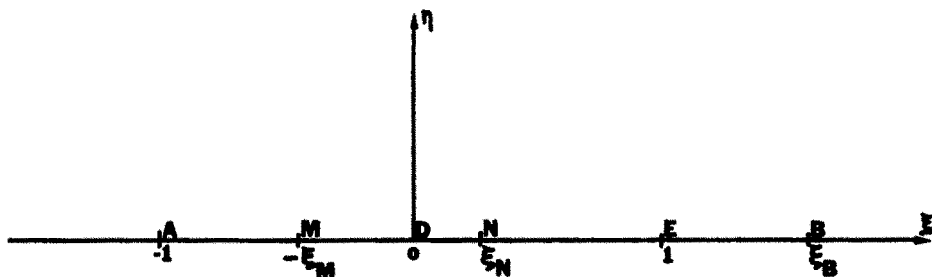Fig 3 The γ-plane for symmetric crack bifurcation.

Fig 4 The ζ-plane for symmetric crack bifurcation

the mappings of points D and B:

$$\kappa(1 - \xi_M^2)^{1/2}/\xi_M - (1 - \kappa)(1 - \xi_N^2)^{1/2}/\xi_N = 0, \tag{4.8}$$

$$\gamma_D = \kappa \cosh^{-1}(1/\xi_M) + (1 - \kappa) \cosh^{-1}(1/\xi_N) + i\kappa\pi,$$

$$= \cosh^{-1}(1/m) + i\kappa\pi, \tag{4.9}$$

$$\kappa \sin^{-1}\left(\frac{1 + \xi_B\xi_M}{\xi_B + \xi_M}\right) + (1 - \kappa) \sin^{-1}\left(\frac{1 - \xi_B\xi_N}{\xi_B - \xi_N}\right) = \sin^{-1}\left(\frac{1}{n}\right). \tag{4.10}$$

The physical boundary conditions transform into the following conditions on the real axis in the ζ-plane:

$$-\infty < \xi < -\xi_M: \quad \dot{w} = 0, \qquad \partial\dot{w}/\partial\xi = 0, \tag{4.11}$$

$$-\xi_M < \xi < 1: \qquad \partial\dot{w}/\partial\eta = 0, \tag{4.12}$$

$$1 < \xi < \xi_B: \quad \dot{w} = \frac{(c\tau_0^a/\mu)n}{(n^2 - 1)^{1/2}}, \qquad \frac{\partial\dot{w}}{\partial\xi} = 0, \tag{4.13}$$

$$\xi_B < \xi < \infty: \quad \dot{w} = 0, \qquad \partial\dot{w}/\partial\xi = 0. \tag{4.14}$$

With $\dot{w} = \mathrm{Re}\, F(\zeta)$ and $F'(\zeta) = \partial\dot{w}/\partial\xi - i(\partial\dot{w}/\partial\eta)$, the discontinuity in $\dot{w}$ at ξ_B suggests a simple pole in $F'(\zeta)$ at that point, while the changes in $F'(\zeta)$ from real to imaginary suggest $(\zeta - 1)^{-1/2}(\zeta + \xi_M)^{-1/2}$; in the latter expression negative exponents ensure that points of bounded behavior in the physical plane retain the same boundedness in the ζ-plane. The following expressions satisfy these conditions, as well as the conditions outlined with respect to (2.13):

$$F_1'(\zeta) = \frac{iA^a(\xi_B - 1)^{1/2}(\xi_B + \xi_M)^{1/2}}{(\zeta - 1)^{1/2}(\zeta + \xi_M)^{1/2}(\zeta - \xi_B)}, \tag{4.15}$$

$$F_2'(\zeta) = \frac{iA^a(B^a/\zeta + C^a/\zeta^2)}{(\zeta - 1)^{1/2}(\zeta + \xi_M)^{1/2}}. \tag{4.16}$$

Achenbach[32] formulated the problem under consideration for the particular case $u = \infty$ and $\tau_1^a = 0$ in (4.1) and (4.2), respectively. Unfortunately the analytic function $F'(\zeta)$ chosen by Achenbach[32] did not include $F_2'(\zeta)$ and is thus not complete, as revealed by Burgers and Dempsey[25].

$F_1'(\zeta)$ satisfies the boundary conditions; the jump in particle velocity at $\xi = \xi_B$ gives $A^a = -(c\tau_0^a/\mu\pi)n/(n^2 - 1)^{1/2}$. The integration of $F_2'(\zeta)$ gives rise to an arcsin term which in turn gives rise to a logarithmic singularity in the particle velocity near the crack tip; to exclude this singularity it is necessary that $B^a = C^a(1 - \xi_M)/2\xi_M$. To evaluate the constant C^a observe that the regular part of $\tau_{\theta z}$ in (2.19) for $\theta = \kappa\pi$ and $(r - vt) \to 0^+$ must be equal to the loading on the new crack faces for $\theta = \kappa\pi$ and $(r - vt) \to 0^-$. Thus, for the loading given in (4.2), and noting that C^a is present in $F_2(\zeta)$,

$$F_2(\zeta) = iA^aC^a(\zeta - 1)^{1/2}(\zeta + \xi_M)^{1/2}/\xi_M\zeta, \tag{4.17}$$

and therefore also in $J_{2\theta}$, defined by (2.21), the equation for C^a is given by the regular or nonsingular part of $\tau_{\theta z}$ (2.19) as

$$J_{2\theta}(v, \kappa\pi) + I_{1\theta}(v, \kappa\pi) + \tau_{\theta z}'' = -\tau_1^a. \tag{4.18}$$

By (4.5), $\tau_{\theta z}'' = 0$ for $|\kappa\pi| < \pi/2 + \sin^{-1}(1/n)$.

Before determining the stress intensity factor as defined by (2.22), it is necessary

to calculate the following: immediately ahead of the crack tip $\zeta \sim r\eta$ as $(r - vt) \to 0^+$ on $\theta = \kappa\pi$, where η^2 is determined from (2.11), (2.12) as

$$\eta^2 = 2(r - vt)/vt(1 - m^2)^{1/2}\, \omega_2. \tag{4.19}$$

The constant ω_2 is defined in (2.10) and can be found by expanding (4.7) in a Taylor series about the crack tip $\zeta = 0$; it is found that

$$\omega_2 = \kappa(1 - \xi_M^2)^{1/2}/\xi_M^2 + (1 - \kappa)(1 - \xi_N^2)^{1/2}/\xi_N^2. \tag{4.20}$$

A quick examination of (4.17), (4.19) and (2.19) verifies that the appropriate crack-tip singularity $(r - vt)^{-1/2}$ is indeed present in the first term. Finally, the stress intensity factor is given by

$$K_{\mathrm{III}}^a(\kappa) = \tau_0^a(ct)^{1/2}\, C^a\, \omega_2^{1/2}\, n(1 - m^2)^{3/4}/\{\pi(n^2 - 1)m\xi_M\}^{1/2}, \tag{4.21}$$

where C^a is defined by (4.18).

The mapping in (4.7) can be inverted for two specific cases $\kappa = 0$ and $\kappa = 1/2$; in other words, $\zeta(\kappa = 0)$ and $\zeta(\kappa = 1/2)$ can be written explicitly in terms of s and θ. Analytical solutions are thereby feasible and are presented below. Burgers and Dempsey[25] in a similar treatment obtained analytical solutions for the particular case $u = \infty$ and $\tau_1^a = 0$ in (4.1) and (4.2), respectively.

Consider first the specific case when the crack propagates in its own plane ($\kappa = 0$). The solution of (4.8)–(4.10) gives

$$\kappa = 0: \qquad \xi_M = 0, \quad \xi_N = m, \quad \xi_B = (m + n)/(1 + mn), \tag{4.22}$$

and the inversion of (4.7) gives

$$\kappa = 0: \qquad \zeta = [1 + m\cosh(\gamma - i\pi)]/[m + \cosh(\gamma - i\pi)], \tag{4.23}$$

where $\gamma = \beta + i\theta = \cosh^{-1}(c/s) + i\theta$. For $\theta = 0$ and $r > vt$, (4.23) gives $\zeta = -(s/c - m)/(1 - ms/c)$. From the latter expression it is apparent that $C^a \equiv 0$ in (4.16); otherwise $\tau_{\theta z}$ would be more singular than $(r - vt)^{-1/2}$. In (4.15), A^a has the same value as found previously, while (4.16) gives $F_2(\zeta) = iA^a B^a 2(\zeta - 1)^{1/2}/\zeta^{1/2}$. The final expressions for the shear stress $\tau_{\theta z}$ ahead of the crack tip and the stress intensity factor are obtained from (2.19) and (2.22), respectively, and are

$$\tau_{\theta z}^a(r > vt, \theta = 0) = \left(\frac{2}{\pi}\right)\left\{\left[\tau_0^a\left(\frac{m + n}{1 + n}\right)^{1/2} - (\tau_0^a - \tau_1^a)m^{1/2}\right]\left(\frac{ct - r}{r - vt}\right)^{1/2}\right.$$
$$+ (\tau_0^a - \tau_1^a)\tan^{-1}\left(\frac{t - r/c}{r/v - t}\right)^{1/2}$$
$$\left. - \tau_0^a\tan^{-1}\left[\left(\frac{m + n}{1 + n}\right)^{1/2}\left(\frac{ct - r}{r - vt}\right)^{1/2}\right]\right\}, \tag{4.24}$$

$$K_{\mathrm{III}}^a(\kappa = 0) = 2\left(\frac{2}{\pi}\right)^{1/2}(ct)^{1/2}(1 - m)^{1/2}$$
$$\times \left\{\tau_0^a\left(\frac{m + n}{1 + n}\right)^{1/2} - (\tau_0^a - \tau_1^a)m^{1/2}\right\}. \tag{4.25}$$

For $u \to \infty$ and appropriate values for τ_0^a and τ_1^a the expressions (4.24) and (4.25) agree with those found for three different loading cases examined by Burgers and Dempsey[25]. From energy considerations, the stress intensity factor in (4.21) as $\kappa \to 0$ is expected to be $2^{-1/2}$ times that given in (4.25); that is, $K_{\mathrm{III}}^a(\kappa \to 0) = K_{\mathrm{III}}^a(\kappa = 0)/2^{1/2}$.

For crack branching normal to the primary crack plane ($\kappa = 1/2$), the mapping equations (4.8)–(4.10) give

$$\kappa = 1/2: \qquad \xi_M = \xi_N = m, \quad \xi_B = h = \{n^2(1 - m^2) + m^2\}^{1/2}, \qquad (4.26)$$

and the inversion of (4.7) gives

$$\kappa = 1/2: \qquad \zeta^2 = 1 - (1 - m^2)\tanh^2(\gamma - i\pi). \qquad (4.27)$$

Ahead of the crack tip ($\theta = \pi/2$, $r > vt$) (4.27) gives $\zeta = i(s^2/c^2 - m^2)^{1/2}/(1 - s^2/c^2)^{1/2}$; the latter expression and (4.17) confirm that the appropriate crack-tip singularity is incorporated in $\tau_{\theta z}$ as given by (2.19). The shear stress ahead of the crack tip is given by

$$
\begin{aligned}
\tau_{\theta z}^a\Big|_{\kappa=1/2}\left(r > vt, \theta = \frac{\pi}{2}\right) &= \frac{2^{1/2}}{\pi}\left\{\tau_0^a(1 - m)^{1/2}\left(\frac{h - m}{h + 1}\right)^{1/2}\right. \\
&\quad \left. + \tau_1^a 2^{1/2}m^{1/2}\right\}\left(\frac{ct - r}{r - vt}\right)^{1/2} \\
&\quad + \tau_0^a Y\left\{\tan^{-1}\left[\left(\frac{ct - r}{r - vt}\right)^{1/2}\left(\frac{y + m}{y + 1}\right)^{1/2}\right]\right. \\
&\quad \left. - \tan^{-1}\left[\left(\frac{ct - r}{r - vt}\right)^{1/2}\left(\frac{y - m}{y - 1}\right)^{1/2}\right]\right\} \\
&\quad - \tau_1^a\left(\frac{2}{\pi}\right)\tan^{-1}\left(\frac{t - r/c}{r/v - t}\right)^{1/2}, \qquad (4.28)
\end{aligned}
$$

where

$$Y = \frac{(1 - m)^{1/2}\{(y + m)^{1/2}(y + 1)^{1/2} + (y - m)^{1/2}(y - 1)^{1/2}\}}{\pi 2^{1/2}(h - m)^{1/2}(h + 1)^{1/2}}, \qquad (4.29)$$

in which

$$y = n/(n^2 - 1)^{1/2}. \qquad (4.30)$$

The Mode III elastodynamic stress intensity factor defined in (2.22) is therefore given by

$$K_{III}^a\left(\kappa = \frac{1}{2}\right) = (ct)^{1/2}\left(\frac{2}{\pi^{1/2}}\right)(1 - m)^{1/2}\left\{\tau_0^a(1 - m)^{1/2}\left(\frac{h - m}{h + 1}\right)^{1/2} + \tau_1^a 2^{1/2}m^{1/2}\right\}. \qquad (4.31)$$

Symmetrical deformations

Consider now dynamic loading conditions that cause symmetric deformations about the original crack plane. The boundary conditions for this problem are given by (3.12), (3.14), (3.15) and

$$\theta = \pm\kappa\pi, \quad r > 0: \qquad \tau_{\theta z} = \mp\tau_1^a H(t - r/v). \qquad (4.32)$$

Only a cylindrical wave is generated by this loading.

The upper half of the physical domain ($0 \le \theta \le \pi$, $s < c$) is mapped into a semi-infinite strip ($0 \le \theta \le \pi$, $0 \le \beta < \infty$) in the γ-plane (Fig. 3). The boundary conditions in the γ-plane along EN, DN, DM and AM in Fig. 3 are given by $\partial w/\partial\theta = 0$; along AE,

$\dot{w} = 0$ and $\partial\dot{w}/\partial\theta = 0$. This strip is then mapped to the upper half of the ζ-plane (Fig. 4) by the transformation in (4.7). The boundary conditions in the ζ-plane for $|\xi| \geq 1$, $\eta = 0$ are given by $\dot{w} = 0$ and $\partial\dot{w}/\partial\xi = 0$; for $|\xi| \leq 1$, $\eta = 0$ (*AE*), $\partial\dot{w}/\partial\eta = 0$.

Based on considerations similar to those following (4.11)–(4.14), the following expressions are deduced:

$$F_1'(\zeta) = 0, \tag{4.33}$$

$$F_2'(\zeta) = \frac{iA^s(B^s/\zeta + C^s/\zeta^2)}{(\zeta^2 - 1)^{1/2}}, \tag{4.34}$$

where here A^s is introduced for convenience: $A^s = c\tau_1^s/\mu\pi$. The integration of $F_2'(\zeta)$ gives rise to a term $-iB^s \sin^{-1}(1/\zeta)$, which in turn gives rise to a logarithmic singularity in the particle velocity near the crack tip (that is, as $r - vt \to 0^-$); to exclude this singularity it is necessary that $B^s = 0$. The final expression for $F_2(\zeta)$ is

$$F_2(\zeta) = iA^sC^s(\zeta^2 - 1)^{1/2}/\zeta. \tag{4.35}$$

The evaluation of C^s follows from the fact that the nonsingular part of $\tau_{\theta z}$ in (2.19) for $\theta = \kappa\pi$ and $(r - vt) \to 0^+$ must equal the loading on the new crack faces for $\theta = \kappa\pi$ and $(r - vt) \to 0^-$. Since $F_1(\zeta) = 0$ and $\tau_{\theta z}^w = 0$ for $|\theta| \leq \pi$ by (3.14), the equation used to determine C^s quickly follows from (2.19) and (4.32) as

$$J_{2\theta}(v, \kappa\pi) = -\tau_1^s. \tag{4.36}$$

Ahead of the crack tip ($\theta = \kappa\pi$, $r > vt$) $\zeta \sim i\eta$, where η^2 is again given by (4.19) and (4.20). The first term in (2.19), the definition (2.22), and the expression for $F_2(\zeta)$ in (4.35) are used to determine that

$$K_{\text{III}}^s(\kappa) = \tau_1^s(ct)^{1/2}C^s\omega_2^{1/2}(1 - m^2)^{3/4}/(\pi m)^{1/2}. \tag{4.37}$$

For crack branching normal to the primary crack plane ($\kappa = 1/2$), (4.7) can be inverted to give (4.27), and an analytical solution can be obtained. From (4.36) it is determined that

$$C^s = -\pi m^2/qE(q), \tag{4.38}$$

where $q = (1 - m^2)^{1/2}$. The final expressions for the stress ahead of the crack tip and the stress intensity factor are found from (2.19) and (4.37), respectively, as

$$\tau_{\theta z} \left.\left(r > vt, \theta = \frac{\pi}{2}\right)\right|_{\kappa = 1/2} = \tau_1^s \frac{\{(r/ct)(c^2t^2 - r^2)^{1/2}/(r^2 - v^2t^2)^{1/2} - E(\lambda, q)\}}{E(q)}, \tag{4.39}$$

in which $\lambda = \sin^{-1}\{(c^2t^2 - r^2)^{1/2}/(r^2 - v^2t^2)^{1/2}\}$, and

$$K_{\text{III}}^s(\kappa = 1/2) = \tau_1^s(ct)^{1/2}\pi^{1/2}m^{1/2}(1 - m^2)^{1/2}/E(q). \tag{4.40}$$

In the above expressions, $E(\cdot)$ and $E(\cdot, \cdot)$ are, respectively, complete and incomplete elliptic integrals of the second kind (Gradshteyn and Ryzhik[38]).

It is worthwhile at this point to consider for a moment the antiplane strain problem of skew crack propagation into a half-plane ($-\infty < x < \infty$, $0 < y < \infty$) at an angle $\theta = \kappa\pi$ with the loading: $\tau_{\theta z} = \mp\tau_1^s$ for $0 < r < vt$, and $\tau_{\theta z} = 0$ on $\theta = 0$, π for $r > 0$. Obviously, these boundary conditions are identical to those stated for the symmetrical bifurcation problem with symmetrical deformations that has just been examined here. Therefore, the expressions in (4.35) and (4.37) apply equally to the problem just described.

Symmetric crack bifurcation under stress wave loading

The problem of crack bifurcation under stress wave loading is discussed in Section 3. The Mode III elastodynamic stress intensity factors for the superposition problem shown in Fig. 2(b) and defined in eqns (3.4)–(3.6) are quickly obtained for symmetric crack bifurcation with equal crack-tip velocities. In this instance, the solutions of the antisymmetric and symmetric problems defined in Section 3 are required. These solutions are provided in this section, and by comparing (3.4) and (3.10) with (4.1) and (4.2), respectively, as well as (3.13) with (4.32), it is immediate that

$$K_{III}^D(\kappa) = K_{III}^a(\kappa) + K_{III}^s(\kappa), \tag{4.41}$$

and

$$K_{III}^C(\kappa) = K_{III}^a(\kappa) - K_{III}^s(\kappa), \tag{4.42}$$

so long as $\tau_0^a = \tau_0 \cos(\alpha\pi)$, $\tau_1^a = \tau_0 \cos(\alpha\pi) \cos(\kappa\pi)$, $\tau_1^s = \tau_0 \sin(\alpha\pi) \sin(\kappa\pi)$, and $n = 1/\sin(\alpha\pi)$. The analytical solutions $K_{III}^a(\kappa = 1/2)$ and $K_{III}^s(\kappa = 1/2)$ provided in (4.31) and (4.40), respectively, provide in turn analytical expressions for $K_{III}^D(\kappa = 1/2)$ and $K_{III}^C(\kappa = 1/2)$. A noteworthy feature of the above information is that for normal incidence

$$\alpha = 0: \qquad K_{III}^D(\kappa) = K_{III}^C(\kappa) = K_{III}^a, \tag{4.43}$$

with $\tau_0^a = \tau_0$, $\tau_1^a = \tau_0 \cos(\kappa\pi)$, $\tau_1^s = 0$ and $n \to \infty$; for grazing incidence

$$\alpha = 0.5: \qquad K_{III}^D(\kappa) = - K_{III}^C(\kappa) = K_{III}^s(\kappa), \tag{4.44}$$

with $\tau_0^a = \tau_1^a = 0$, $\tau_1^s = \tau_0 \sin(\kappa\pi)$ and $n = 1$. The dependence of the elastodynamic
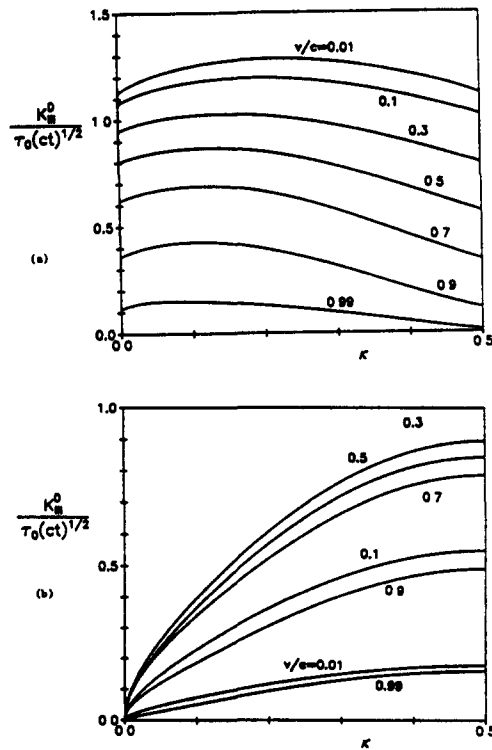

Fig. 5. Symmetric crack bifurcation ($\kappa_1 = -\kappa_2 = \kappa$, $v_1 = v_2 = v$): (a) $\alpha = 0$ (normal incidence), $K_{III}^D = K_{III}^C$ vs κ; (b) $\alpha = 0.5$ (grazing incidence), $K_{III}^D = -K_{III}^C$ vs κ.
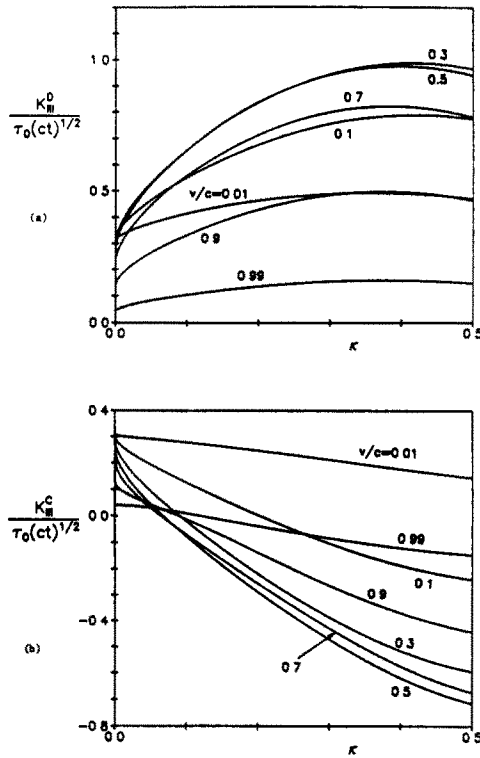
Fig 6 Symmetric crack bifurcation ($\kappa_1 = -\kappa_2 = \kappa$, $v_1 = v_2 = v$), $\alpha = 0.375$ (a) K^D_{III} vs κ, (b) K^C_{III} vs κ.

stress intensity factors stated in (4.43) and (4.44) on the angle of branching ($\kappa\pi$) is shown in Fig. 5 for different values of $m = v/c$. The dependence of $K^D_{III}(\kappa)$ and $K^C_{III}(\kappa)$ as stated in (4.41) and (4.42) is shown in Fig. 6 for $\alpha = 0.375$.

5 ASYMMETRIC CRACK BIFURCATION

The superposition problem defined in (3.4)–(3.6) is now examined for geometrically asymmetric bifurcation and different crack propagation velocities. As outlined in Sec-
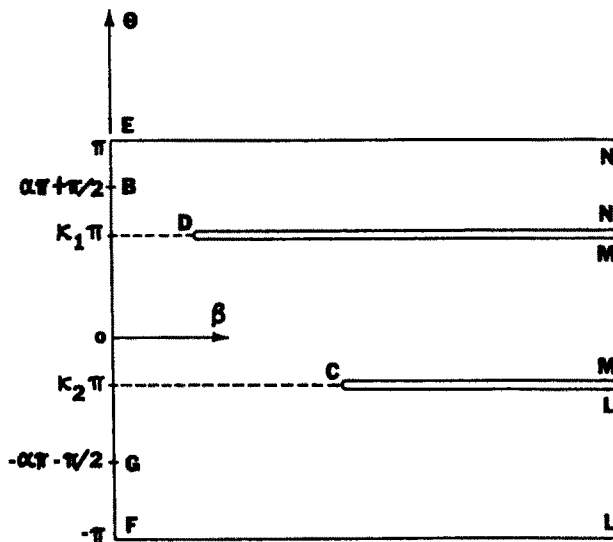

Fig. 7. The γ-plane for asymmetric crack bifurcation. The boundary conditions along EN, DN, DM, CM, CL and FL are given by $\partial \dot{w}/\partial\theta = 0$; along FG, $\dot{w} = -c\tau_0/\mu$; along GB, $\dot{w} = 0$, along BE, $\dot{w} = c\tau_0/\mu$.
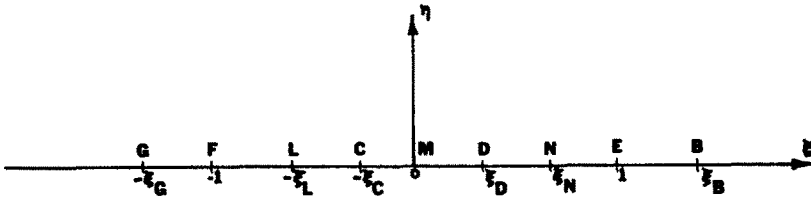
Fig. 8. The ζ-plane for asymmetric crack bifurcation The boundary conditions along $EBGF$ are given by $\partial w/\partial\xi = 0$; along $FLCMDNE$ $\partial w/\partial\eta = 0$

tion 2 this asymmetric problem is mapped from the physical domain ($-\pi \leq \theta \leq \pi$, $s \leq c$) into a semi-infinite strip ($-\pi \leq \theta \leq \pi$, $0 \leq \beta < \infty$) in the γ-plane (Fig. 7). This strip is then mapped to the upper half of the ζ-plane (Fig. 8) by the Schwarz–Christoffel transformation (Kuo[39])

$$\gamma = (\kappa_1 - \kappa_2) \cosh^{-1}\left(\frac{1}{\zeta}\right) + (1 - \kappa_1) \cosh^{-1}\left(\frac{1 - \xi_N\zeta}{\zeta - \xi_N}\right)$$

$$+ (1 + \kappa_2) \cosh^{-1}\left(\frac{1 + \xi_L\zeta}{\zeta + \xi_L}\right) + i\pi, \tag{5.1}$$

where the points ξ_L, ξ_N, ξ_C, ξ_D, ξ_B and ξ_G can be found for given values of κ_1, κ_2, v_1/c and v_2/c by examining the changes in imaginary parts at L, M and N and from the mappings of points B, C, D and G.

In the ζ-plane the boundary condition on $\dot{w}(\xi, \eta)$ corresponding to those in the γ-plane are, at $\eta = 0$:

$$- \infty < \xi < -\xi_G: \quad \dot{w} = 0, \qquad \partial\dot{w}/\partial\xi = 0, \tag{5.2}$$

$$- \xi_G < \xi < - 1: \quad \dot{w} = - c\tau_0/\mu, \quad \partial\dot{w}/\partial\xi = 0, \tag{5.3}$$

$$- 1 < \xi < 1: \quad \partial\dot{w}/\partial\eta = 0, \tag{5.4}$$

$$1 < \xi < \xi_B: \quad \dot{w} = c\tau_0/\mu, \qquad \partial\dot{w}/\partial\xi = 0, \tag{5.5}$$

$$\xi_B < \xi < \infty: \quad \dot{w} = 0, \qquad \partial\dot{w}/\partial\xi = 0. \tag{5.6}$$

The discontinuities in $\dot{w}$ at $\xi = -\xi_G$ and $\xi = \xi_B$ suggest simple poles in $F'(\zeta)$ at these points, while the changes in $F'(\zeta)$ from real to imaginary along $| \xi | \leq 1$ indicate that the term $(\zeta^2 - 1)^{-1/2}$ is needed. The following expressions satisfy the above conditions and incorporate the singular behavior at the two crack tips:

$$F_1'(\zeta) = \frac{iA}{(\zeta^2 - 1)^{1/2}} \left[\frac{(\xi_G^2 - 1)^{1/2}}{\zeta + \xi_G} + \frac{B(\xi_B^2 - 1)^{1/2}}{\zeta - \xi_B} \right], \tag{5.7}$$

$$F_2'(\zeta) = \frac{iA}{(\zeta^2 - 1)^{1/2}} \left[\frac{E}{\zeta - \xi_D} + \frac{D}{(\zeta - \xi_D)^2} + \frac{H}{\zeta + \xi_C} + \frac{G}{(\zeta + \xi_C)^2} \right]. \tag{5.8}$$

Achenbach[31] formulated a similar problem to that considered above. Unfortunately, the analytic function $F'(\zeta)$ chosen in [31] did not include $F_2'(\zeta)$, thus precluding a complete analysis.

The task remaining is to determine the constants A, B, D, E, G, H such that the conditions stated in (3.4)–(3.9) and in (5.2)–(5.6) are satisfied. After eqns (5.7) and (5.8) are integrated, the conditions $\dot{w} = -c\tau_0/\mu$ for $-\xi_G < \xi < -1$, $\dot{w} = c\tau_0/\mu$ for $1 < \xi < \xi_B$ determine that $A = c\tau_0/\mu\pi$ and $B = -1$. To preclude terms giving rise to logarithmic singularities in the particle velocity in the vicinity of the crack tips, it is necessary that $D\xi_D/(1 - \xi_D^2) + E = 0$ and $G\xi_C/(1 - \xi_C^2) - H = 0$. The latter conditions

negate any arcsin terms in $F_2(\zeta)$, which is finally given by

$$F_2(\zeta) = iA(\zeta^2 - 1)^{1/2}\{D/(1 - \xi_D^2)(\zeta - \xi_D) + G/(1 - \xi_C^2)(\zeta + \xi_C)\}. \qquad (5.9)$$

The remaining constants D and G have to be determined on the basis of considerations of the shear stress $\tau_{\theta z}$ in the plane of, and ahead of, each crack tip. The regular part of $\tau_{\theta z}$ in (2.19) for $(r - v_1 t) \to 0^+$, $\theta = k_1\pi$, for instance, must be equal to the loading on the new crack face for $(r - v_1 t) \to 0^-$, $\theta = \kappa_1\pi$ (the medium ahead of BG in the superposition problem is undisturbed; therefore $\tau_{\theta z}^w = 0$ for the range of branching angles considered). Thus, noting (2.19), (2.21), (2.15), (5.9), (3.5) and (3.6), it is found that for $\theta_1 = \kappa_1\pi$ and $\theta_2 = \kappa_2\pi$

$$J_{2\theta}(v_p, \kappa_p\pi) + I_{1\theta}(v_p, \kappa_p\pi) = -\tau_0 \cos(\alpha\pi - \kappa_p\pi) \qquad (p = 1, 2), \qquad (5.10)$$

where it is to be noted from (5.9) that the constants D and G are present in $J_{2\theta}$; (5.10) gives two equations in these two unknowns. The elastodynamic Mode III stress intensity factors follow from the singular part of the stress (2.19) in the planes $\theta_1 = \kappa_1\pi$ and $\theta_2 = \kappa_2\pi$, respectively. Noting (2.22) we find that

$$K_{III}^D = -\tau_0(ct)^{1/2} D[\omega_2^D(1 - m_1^2)^{3/2}/\pi m_1(1 - \xi_D^2)]^{1/2}, \qquad (5.11)$$

$$K_{III}^C = -\tau_0(ct)^{1/2} G[\omega_2^C(1 - m_2^2)^{3/2}/\pi m_2(1 - \xi_C^2)]^{1/2}, \qquad (5.12)$$

in which $m_p = v_p/c$ $(p = 1, 2)$ and ω_2^D for this problem [see (2.10)] is given by

$$\omega_2^D = \frac{1}{(1 - \xi_D^2)^{1/2}}\left[\frac{\kappa_1 - \kappa_2}{\xi_D^2} + \frac{(1 - \kappa_1)(1 - \xi_N^2)^{1/2}}{(\xi_N - \xi_D)^2} + \frac{(1 + \kappa_2)(1 - \xi_L^2)^{1/2}}{(\xi_L + \xi_D)^2}\right], \qquad (5.13)$$
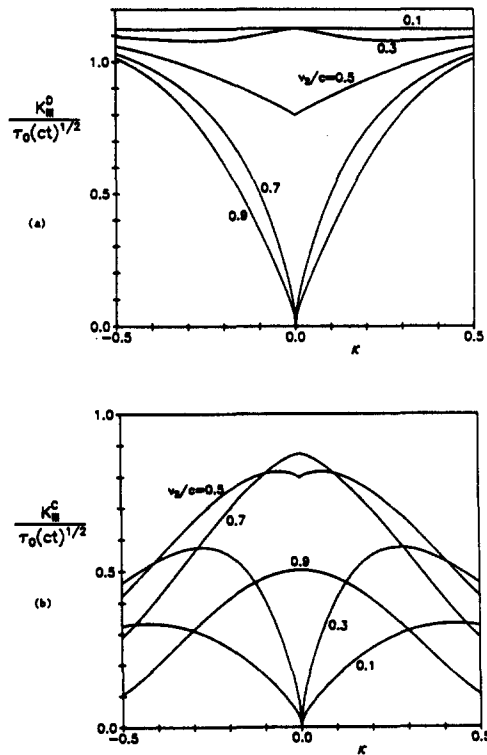

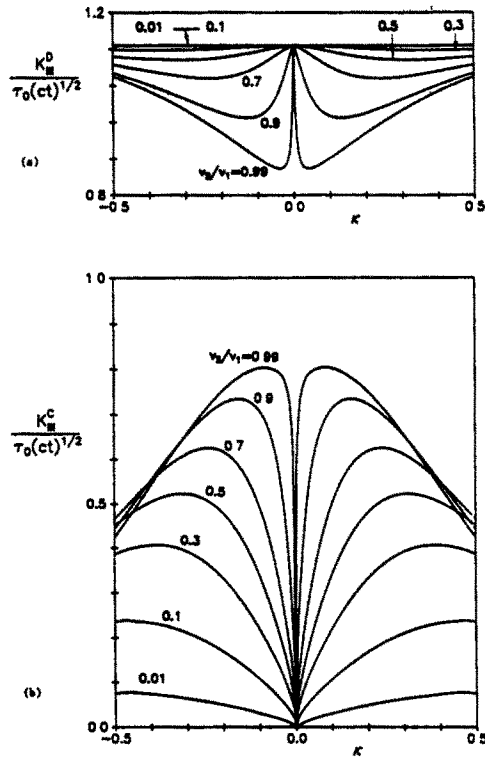Fig. 9. Asymmetric crack bifurcation with $\kappa_1 = 0$, $\kappa_2 = \kappa$, $v_1/c = 0.5$ and $\alpha = 0$ (normal incidence): (a) K_{III}^D vs κ for different values of v_2/c; (b) K_{III}^C vs κ for different values of v_2/c.

Fig. 10. Asymmetric crack bifurcation with $\kappa_1 = 0$, $\kappa_2 = \kappa$, $v_1/c = 0.5$, and $\alpha = 0$ (normal incidence): (a) K_{III}^D vs κ for different values of v_2/v_1; (b) K_{III}^C vs κ for different values of v_2/v_1.

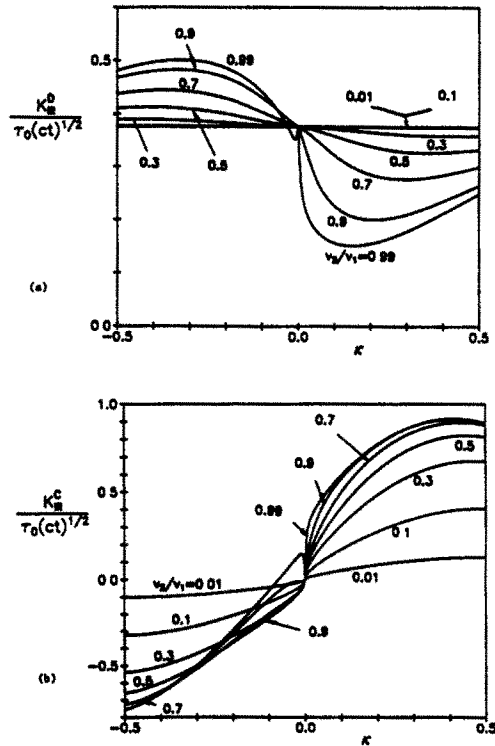Fig. 11. Asymmetric crack bifurcation with $\kappa_1 = 0$, $\kappa_2 = \kappa$, $v_1/c = 0.5$, and $\alpha = 0.375$. (a) K_{III}^D vs κ for different values of v_2/v_1; (b) K_{III}^C vs κ for different values of v_2/v_1.

while the equivalent expression for ω_2^C is the same as (5.13), except that ξ_D must be replaced by $-\xi_C$.

The dependence of the stress intensity factors K_{III}^D and K_{III}^C on the two crack-tip velocities, the two branching angles, and the angle of wave incidence is now investigated. A general analysis is not possible. Rather, the sensitivity of one branch's crack-tip stress intensity factor to the relative velocity and orientation of the other is examined here. The particular geometry chosen is that of $\kappa_1 = 0$ and $\kappa_2 = \kappa$ [see Fig. 2(b)]; the fact that a propagating crack makes several usually abortive crack branching attempts after reaching a certain stress intensity prompted this choice.

In Figs 9 and 10 crack-tip D models the continued planar propagation of the primary crack at a velocity of $v_1 = 0.5c$ under normal wave incidence ($\alpha = 0$). Crack-tip C models the attempted branching. The role played by a nonzero angle of wave incidence is shown in Fig. 11.

6 CONCLUSIONS

For symmetric crack bifurcation Burgers[27] numerically solved the following anti-symmetrical problems—referring to (4.1) and (4.2)—*Case* 1: $\tau_0^u = \tau_0$, $\tau_1^u = 0$, $u \to \infty$; *Case* 2: $\tau_0^u = 0$, $\tau_1^u = \tau_0$; *Case* 3: stress wave loading with normal incidence. The results obtained in [27] revealed that the stress intensity factor $K_{III}^u(\kappa)$ in (4.21) for loading Case 1 reaches a maximum with $\kappa = 1/2$ for all velocities. By eqns (4.31) and (4.43), $K_{III}^D = K_{III}^u = \tau_0(ct)^{1/2}2(1 - m)/\pi^{1/2}$ in this instance. Achenbach[32] treated loading Case 1 also and used his solution to examine the bifurcation of a propagating crack. A reinvestigation of the running crack analysis in [32], after noting that his stress intensity factor K is defined here by $(\pi K/c\tau_0) \equiv K_{III}^u \pi^{1/2} m^{1/2}/\tau_0(ct)^{1/2}(1 - m^2)^{1/4}$, gives different results for the velocity at which bifurcation occurs and the angle of bifurcation, *viz.* $0.6c$ and $\pi/2$, respectively.

For asymmetric crack bifurcation under stress wave loading, Figs 9 and 10 reveal that the stress intensity factor of the unbranched crack-tip D is not significantly influenced if the branching velocities of crack-tip C are less than its own velocity ($0.5c$); for branching velocities of crack-tip C greater than that of the crack-tip D propagating in a planar fashion, K_{III}^D is greatly decreased. A branch cannot propagate almost parallel to the primary crack unless it has a velocity *exactly* equal to that of the primary crack. If the branching velocity is greater than that of the primary crack and small branching angles are involved, K_{III}^D is significantly reduced.

The above study is similar in spirit to that of the elastostatic investigations in [17, 34]. The conclusion here is that continuous branching with very little crack speed alteration is *key* to successful crack branching. From Fig. 9(b), K_{III}^C has two maxima for a crack-tip velocity equal to that of crack-tip D ($v_1 = v_2 = 0.5c$), which suggests that bifurcation, with continued planar crack propagation also, would occur in the model studied (for normal wave incidence) at $\pm 12°$. The amazingly sensitive interaction displayed in the above antiplane strain studies is likely to be a feature also of plane strain crack bifurcation.

REFERENCES

1. H. Schardin, Velocity effects in fracture. In *Fracture* (Edited by B. I. Averbach, D K. Felbeck, G T Hahn and D. A. Thomas), pp. 297–330 The M.I.T. Press, Cambridge, Mass. (1959)
2. A-B. J. Clark and G. R. Irwin, Crack-propagation behaviors. *Exp. Mech.* **6**, 321–330 (1966).
3. J. W. Dally, Dynamic photoelastic studies of fracture. *Exp. Mech.* **19**, 349–361 (1979)
4. K. Ravi-Chandar and W. G Knauss, An experimental investigation into dynamic fracture. III. A steady state crack propagation and crack branching. *Int. J. Fract.* **26**, 141–154 (1984)
5. S. Aoki and M. Sakata, Crack propagation behaviors of glass. In *Symp. of Mechanical Behavior of Materials*, 11–8(1). Soc. Mat. Sci (Japan), Kyoto (1974)

6   G T. Hahn, R G Hoagland and A. R. Rosenfield, Crack branching in A 533B Steel In *Fracture*, Vol 2, pp 1333–1338. University of Waterloo Press (1977)

7   J Congleton, Practical applications of crack-branching measurements In *Dynamic Crack Propagation* (Edited by G C Sih), pp 427–438 Noordhoff, Leyden (1973)

8   A S Kobayashi, Crack branching, crack arrest, and rapid tearing In *Proc Workshop on Dynamic Fracture* California Institute of Technology, Pasadena (1983)

9   J E Field, Brittle fracture its study and application *Contemp Phys* **12**, 1–31 (1971)

10 Z T Bienawski, Fracture dynamics of rock *Int. J. Fracture* **4**, 415–430 (1968).

11 A S Kobayashi, B. G. Wade, W B Bradley and S. T. Chiu, Crack branching in Homelite-100 sheets, *Engng Fracture Mech* **6**, 81–92 (1974)

12. M. Ramulu, A. S. Kobayashi and B. S.-J Kang, Dynamic crack branching—a photoelastic evaluation In *15th Nat Symp. on Fracture Mechanics*. July 7–9 (1982)

13 G C Sih, Stress distributions near internal crack tips for longitudinal problems. *J Appl Mech*. **32**, 51–58 (1965).

14 E. Smith, Crack bifurcation in brittle solids *J. Mech Phys. Solids* **16**, 329–336 (1968).

15. K K. Lo, Analysis of branched cracks *J. Appl Mech*. **45**, 797–802 (1978).

16 W K. Wilson and J. Cherepko, Analysis of cracks with multiple branches. *Int. J. Fracture* **22**, 303–315 (1983)

17 L. G. Parletun, Determination of the growth of branched cracks by numerical methods *Engng Fracture Mech* **11**, 343–358 (1979).

18 N V. Banichuk, Determination of the form of a curvilinear crack by small parameter technique. *Izv AN SSR, MIT* **7**, 130–137 (1970) (in Russian).

19. B. Cotterell and J. R. Rice, Slightly curved or kinked cracks, *Int. J. Fracture* **16**, 155–169 (1980).

20 B L. Karihaloo, L. M. Keer, S Nemat-Nassar and A. Oranratnachai, Approximate description of crack kinking and curving. *J Appl. Mech*. **48**, 515–519 (1981).

21 S. K Maiti and R. A. Smith, Criteria for brittle fracture in biaxial tension. *Engng Fracture Mech* **19**, 793–804 (1984).

22. E H Yoffe, The moving Griffith crack. *Phil Mag*. **42**, 739–750 (1951).

23 J. W. Craggs, On the propagation of a crack in an elastic–brittle material. *J. Mech. Phys. Solids* **8**, 66–75 (1960).

24 N. I. Muskhelishvili, *Some Basic Problems of the Mathematical Theory of Elasticity* (Translated by J. R M. Radok) Noordhoff, Leyden (1977)

25 P. Burgers and J. P Dempsey, Two analytical solutions for dynamic crack bifurcation in antiplane strain. *J Appl Mech* **49**, 366–370 (1982)

26 J P Dempsey, M. K Kuo and J. D. Achenbach, Mode-III crack kinking under stress wave loading *Wave Motion* **4**, 181–190 (1982).

27. P. Burgers, Dynamic propagation of a kinked or bifurcated crack in antiplane strain *J. Appl. Mech* **49**, 371–376 (1982)

28 P Burgers, Kinking of a crack in plane strain, *Int. J. Solids Struct*. **19**, 735–752 (1983).

29 P Burgers and J P. Dempsey, Plane strain dynamic crack bifurcation, *Int. J. Solids Struct*. **20**, 609–618 (1984)

30. J D Achenbach and V. K. Varatharajulu, Skew crack propagation at the diffraction of a transient stress wave *Q. Appl. Math*. **32**, 123–135 (1974)

31. J. D Achenbach, Elastodynamic stress intensity factors for a bifurcating crack. In *Prospects of Fracture Mechanics* (Edited by G C. Sih, H. C. van Elst and D. Broek), pp. 319–336. Noordhoff, Leyden (1974).

32. J. D. Achenbach, Bifurcation of a running crack in antiplane strain. *Int. J. Solids Struct*. **11**, 1301–1314 (1975).

33 L. B Freund, Bifurcation of a propagating crack in a brittle solid. In *Annual Meeting, Soc. Engng Sci*. pp. 1015–1022. University of Texas Press, Austin (1975).

34. J. F Kalthoff, On the propagation direction of bifurcated cracks. In *Dynamic Crack Propagation* (Edited by G C Sih) pp 449–458. Noordhoff, Leyden (1973).

35. F Erdogan, Crack-propagation theories In *Fracture* (Edited by H. Liebowitz), Vol. 2, pp. 497–590. Academic Press, New York (1968)

36 L B. Freund and R. J. Clifton, On the uniqueness of plane elastodynamic solutions for running cracks *J Elasticity* **4**, 293–299 (1974)

37 L B Freund, Energy flux into the tip of an extending crack in an elastic solid. *J. Elasticity* **2**, 341–349 (1972)

38. I S Gradshteyn and I. M. Ryzhik, *Tables of Integrals, Series and Products*. Academic Press, New York (1980).

39 M.-K. Kuo, *Crack kinking and crack forking under stress wave loading*. Ph.D. Thesis, Northwestern University, Evanston, IL (1984).